

## *lin-35/Rb* and the CoREST ortholog *spr-1* coordinately regulate vulval morphogenesis and gonad development in *C. elegans*

Aaron M. Bender<sup>a</sup>, Natalia V. Kirienko<sup>a</sup>, Sara K. Olson<sup>b</sup>, Jeffery D. Esko<sup>b</sup>, David S. Fay<sup>a,\*</sup>

<sup>a</sup> University of Wyoming, College of Agriculture, Department of Molecular Biology, Department 3944, 1000 E. University Avenue, Laramie, WY 82071, USA  
<sup>b</sup> Department of Cellular and Molecular Medicine, Glycobiology Research and Training Center, University of California, San Diego, La Jolla, CA 92093, USA

Received for publication 18 July 2006; revised 28 August 2006; accepted 30 September 2006

Available online 5 October 2006

### Abstract

Using a genetic screen to identify genes that carry out redundant functions during development with *lin-35/Rb*, the *C. elegans* Retinoblastoma family ortholog, we have identified a mutation in *spr-1*. *spr-1* encodes the *C. elegans* ortholog of human CoREST, a protein containing Myb-like SANT and ELM2 domains, which functions as part of a transcriptional regulatory complex. CoREST recruits mediators of transcriptional repression, including histone deacetylase, and demethylase, and interacts with the tumor suppression protein REST. *spr-1/CoREST* was previously shown in *C. elegans* to suppress defects associated with loss of the presenilin *sel-12*, which functions in the proteolytic processing of LIN-12/Notch. Here we show that *lin-35* and *spr-1* coordinately regulate several developmental processes in *C. elegans* including the ingression of vulval cells as well as germline proliferation. We also show that loss of *lin-35* and *spr-1* hypersensitizes animals to a reduction in LIN-12/Notch activity, leading to the generation of proximal germline tumors. This defect, which is observed in *lin-35; spr-1; lin-12(RNAi)* and *lin-35; spr-1; hop-1(RNAi)* triple mutants is likely due to a delay in the entry of germ cells into meiosis.

© 2006 Elsevier Inc. All rights reserved.

**Keywords:** *lin-35*; Retinoblastoma; *spr-1*; CoREST; *C. elegans*; Development

### Introduction

The mammalian pocket proteins, which include the Retinoblastoma protein pRb and its paralogs, p107 and p130, are well-established regulators of the cell cycle (reviewed by Kaelin, 1999; Harbour and Dean, 2000a; Classon and Dyson, 2001). In addition, numerous studies have implicated Rb family members in promoting cell differentiation as well as other processes related to development (reviewed by Harbour and Dean, 2000b; Morris and Dyson, 2001; Wikenheiser-Brokamp, 2006). Although much of the evidence in support of a role for the pocket proteins in development has been obtained from tissue culture-based systems, in vivo results have also provided several notable findings. For example, disruption of Rb family functions in the developing murine lung leads to increased expression of the neuroendocrine cell fate and a concomitant reduction in the specification of other epithelial

cell types, suggesting that Rb family proteins control the development of specific cell lineages within the lung (Wikenheiser-Brokamp, 2004). Furthermore, a role for Rb proteins in skin epithelial cell differentiation is supported by findings that ablation of p107 and p130 results in the impaired differentiation of keratinocytes (Ruiz et al., 2003). Interestingly, this study also revealed an apparent role for p107/p130 in the morphogenesis of epidermal hair follicles and incisors, which is independent of differentiation.

The extent to which these observed developmental defects are an indirect consequence of perturbations to the cell cycle is not entirely clear. Nevertheless, a number of recent in vivo findings support the idea that Rb family activities, including those connected to proliferation, differentiation, and apoptosis, may be functionally separable (de Bruin et al., 2003; MacPherson et al., 2003; Wu et al., 2003; Takahashi et al., 2004; Sage et al., 2005). This separation of functions is further supported at the mechanistic level by the recent finding that the RET finger protein (RFP) specifically inhibits gene transcriptional activation by pRb, but does not inhibit the repressive (cell

\* Corresponding author. Fax: +1 307 766 5098.

E-mail address: [davidfay@uwyo.edu](mailto:davidfay@uwyo.edu) (D.S. Fay).

cycle) functions of pRb (Krutzfeldt et al., 2005). Furthermore, microarray analyses suggest that the transcriptional targets of Rb family proteins as well as their well-established DNA-binding regulatory partners, the E2Fs, include many non-cell cycle targets such as factors implicated in differentiation, signaling, and cell architecture (e.g., Muller et al., 2001; Markey et al., 2002; Polager et al., 2002; Black et al., 2003; Dimova et al., 2003; Balciunaite et al., 2005).

Further evidence in support of a role for the Rb and E2F family proteins in basic developmental functions includes studies from non-mammalian systems. For example, in *Drosophila*, loss of the E2F co-partner dDP results in ventralization of the embryo because of misexpression of the EGF-like ligand Gurkin (Myster et al., 2000). Conversely in *Xenopus*, loss of E2F function leads to the elimination of posterior and ventral structures, whereas overexpression inhibits the formation of dorsal and anterior structures (Suzuki and Hemmati-Brivanlou, 2000). A Role for E2F and Dp in establishing proper body axis patterning is also observed in *C. elegans*, where the loss of these orthologs leads to an early defect in the proper distribution of tissue-specific transcriptional regulators (Page et al., 2001).

Studies on the *C. elegans* Rb family ortholog, *lin-35*, have revealed both canonical cell cycle functions as well as many unexpected roles during development that appear in most cases to be unlinked to cell cycle regulation (reviewed by Fay, 2005). Interestingly, the majority of these functions cannot be detected through the analysis of *lin-35* single mutants. Rather these functions are revealed only when *lin-35* is inactivated in the appropriate mutant backgrounds, indicating that *lin-35* functions redundantly with other pathways to regulate both cell cycle and non-cell cycle processes. This precedent for redundancy of *lin-35* functions was initiated by the discovery of a role for *lin-35* in inhibiting epidermal cells from inappropriately acquiring vulval cell fates (the synthetic multi-vulval [SynMuv] phenotype; Ferguson and Horvitz, 1989; Lu and Horvitz, 1998; reviewed by Fay and Han, 2000), a function that it shares with the *C. elegans* E2F ortholog, *efl-1* (Ceol and Horvitz, 2001). Namely, animals that are mutant for *lin-35* (or other members of the so-called Class B group of SynMuv genes) and for genes of either the Class A (Ferguson and Horvitz, 1989) or Class C (Ceol and Horvitz, 2004) groups show a highly penetrant hyperinduction of vulval cells. The basis for this phenotype was recently shown to be the result of ectopic expression of LIN-3, the EGF-like ligand that is the primary inducer of vulval cell fates (Cui et al., 2006). Further studies looking for novel *lin-35* synthetic phenotypes have revealed roles for LIN-35 in morphogenesis of the *C. elegans* pharynx (Fay et al., 2003, 2004), asymmetric cell divisions (Cui et al., 2004), execution of cell lineages within the somatic gonad (Bender et al., 2004), and larval growth (Cui et al., 2004; Cardoso et al., 2005; Chesney et al., 2006; Fay lab unpublished data), as well as a traditional role in cell cycle control (Boxem and van den Heuvel, 2001, Fay et al., 2002). *lin-35* also functions non-redundantly to repress the expression of germline-associated genes in somatic cells and *lin-35* mutants show hypersensitivity to RNAi (Wang et al., 2005). Finally, *lin-35*

negatively regulates ribosome biogenesis at the level of rRNA expression (Voutev et al., 2006).

In this work, we describe a novel role for *lin-35* in the morphogenesis of the *C. elegans* vulva. Specifically, in double mutants of *lin-35* and the *C. elegans* CoREST transcriptional repressor ortholog, *spr-1*, cells of the vulval epithelium fail to fully ingress, leading to an abnormally compressed vulval lumen at the L4 larval stage. Furthermore, this phenotype does not appear to result from primary defects in either cell cycle regulation or differentiation. We also show a role for *lin-35* and *spr-1* in promoting germline proliferation and in inhibiting the formation of proximal germline tumors. Interestingly, human CoREST is a key cofactor of the REST tumor suppressor gene (Andres et al., 1999; Westbrook et al., 2005). Based on these and other findings, we suggest that the non-cell cycle functions of Rb family members may contribute to the tumor-suppressing activities of these proteins.

## Materials and methods

### *C. elegans* genetic methods and strains

All *C. elegans* strains were maintained according to standard methods (Stiernagle, 2005). All experiments were carried out at 20°C. Strains used in these studies include the following: N2 (wild type), CB4856, MH1461 [*lin-35(n745)*, *kuEx119*], NH2246 [*ayIs4(egl-17::GFP)*], WY301 [*lin-35(n745)*; *egl-17::GFP*], SU93 [*jcis1(ajm-1::GFP)*], WY334 [*spr-1(fd6)*; *lim-7::GFP*], WY258 [*spr-1(fd6)*], JK2868 [*qIs56(lag-2::GFP)*], MH1317 [*kuls29(egl-13::GFP)*], GS1214 [*sel-12(ar171)*, *unc-1(e538)*], WY329 [*lin-35(n745)*; *lag-2::GFP*], WY298 [*lin-35(n745)*; *ajm-1::GFP*], WY248 [*lin-35(n745)*; *spr-1(fd6)*; *kuEx119*], WY328 [*lin-35(n745)*; *dpy-11(e224)*, *spr-1(fd6)*, *unc-76(e911)*; *kuEx119*], WY294 [*lin-35(n745)*; *spr-1(fd6)*; *lim-7::GFP*; *kuEx119*], WY300 [*lin-35(n745)*; *egl-13::GFP*], WY295 [*hop-1(ar179)*; *spr-1(fd6)*; *unc-76(e911)*], WY251 [*lin-35(n745)*; *spr-1(ar205)*; *kuEx119*], WY249 [*lin-35(n745)*; *spr-1(fd6)*; *ajm-1::GFP*; *kuEx119*], WY296 [*lin-35(n745)*; *sel-12(ar171)*, *unc-1(e538)*], WY326 [*lin-35(n745)*; *spr-1(fd6)*; *sel-12(ar171)*, *unc-1(e538)*], DG1575 [*tnIs6(lim-7::GFP)*], and WY299 [*lin-35(n745)*; *lim-7::GFP*].

### *spr-1/slr-10(fd6)* genetic mapping

Based on the failure of *spr-1(fd6)* to cosegregate with *dpy-11* and *unc-76*, *fd6* was assigned to the right arm of LGV. 59/79 Dpy non-Unc and 14/55 Unc non-Dpy recombinants segregating from *lin-35*; *dpy-11*, *fd6*, *unc-76/+* hermaphrodites retained *fd6*. The genetic region containing *fd6* was further refined by SNP mapping according to standard methods (for details see Fay, 2006). *fd6* was mapped to a 425-kb region on LGV between the polymorphisms *vm23b06.s1@42,a,42* on cosmid F40A3 and *eam66g04.s1@467,t,51* on cosmid F21F8.

### Transgene rescue

Rescue of *fd6* was obtained through the injection of cosmids D1014 and F20D6 together with pRF4 into *lin-35*; *spr-1*; *kuEx119(+)* hermaphrodites (for details on methods see Evans, 2005). Rescue was inferred based on the appearance of roller animals that did not require *kuEx119* for rapid growth or long-term viability. In addition, transgenic rescue was also obtained with YAC Y97E10.

### Complementation test

*spr-1(ar205)* males were crossed to *lin-35(n745)*; *dpy11(e224)*, *spr-1(fd6)*, *unc-76(e911)*; *kuEx119* hermaphrodites and Non-Dpy Unc cross progeny containing the *kuEx119* array were identified in the next generation, clonally transferred, and allowed to self fertilize. 60 non-Dpy Unc *kuEx119+* progeny

were clonally transferred and subsequent generations were analyzed for their dependence on the array. 14/60 (23%; expect 25% based on the expected frequency of *lin-35* homozygous mutants) animals were found to require *kuEx119* for normal health and viability. Of these 14 animals, nine gave rise to small broods containing Dpy Unc animals, indicating that the parental genotype was *lin-35(n745); dpy11(e224), spr-1(fd6), unc-76(e911)/spr-1(ar205); kuEx119*. Analysis of one of the nine balanced isolates revealed vulval morphology and gonad defects similar to those observed for *lin-35(n745); spr-1(fd6)* mutants (data not shown).

#### DAPI staining

Prior to staining, animals were fixed with ice-cold methanol for 5 min in a glass depression slide. Animals were then washed several times with PBS (pH 7.4) containing 0.1% Tween 20. They were then incubated in 0.01 ng/ $\mu$ l DAPI for 1 h at 4°C, washed several times with PBS, and placed on slides for microscopy.

#### Immunohistochemistry

Animals were collected in M9, placed on glass slides coated with poly-L-lysine, and freeze cracked (for details see Duerr, 2005). Slides were blocked with TBS containing 0.1% Tween 80, and animals were treated with 0.05 U/ $\mu$ l chondroitinase ABC for 1 h at 37°C (Mizuguchi et al., 2003). The slides were then washed with TBS and incubated with the 1-B-5 chondroitin stub mAb (1:2000; Seikagaku) for 2–6 h. After washing in TBS, slides were incubated with a Cy3-conjugated donkey anti-mouse secondary antibody (1:1000; Jackson ImmunoResearch) for 2 h. After additional washing with TBS, slides were coated with mounting solution (Dabco) and visualized by fluorescence microscopy.

#### Western blotting

Crude extracts were prepared by sonicating worms in 50 mM NaAc (pH 6) with protease inhibitor cocktail (Sigma). The resulting extract (2  $\mu$ g) was digested with 10 mU chondroitinase ABC (Seikagaku) for 3 h at 37°C and analyzed by SDS-PAGE, as described (Hwang et al., 2003a,b). Chondroitin proteoglycan core proteins were detected by western blotting with the 1-B-5 chondroitin stub mAb (1:1000; Seikagaku) followed by a goat anti-mouse secondary antibody (1:2000; BioRad). Blots were visualized with the WestPico Chemiluminescent Kit (Pierce).

#### RNAi by feeding or microinjection

RNAi feeding and microinjection experiments were carried out according to standard methods (Ahringer, 2005). For microinjection, all dsRNAs were injected into the syncytial germlines of adult hermaphrodites at a concentration of  $\sim$ 1.0  $\mu$ g/ $\mu$ l. Injected animals were allowed to recover for 24 h on NGM plates and were then transferred to fresh plates. F1 self-progeny produced from 24–48 h post-injection were scored for the relevant phenotypes. Forward and reverse primer sequences used to amplify products for RNA were as follows: *spr-1*, ATGGATTTGTATGACGATGATGGA and CTGCATATTTT-CAGCTTTTTCTCCA; *spr-4*, ATGTCGTCGGAACCAACTTCTT and TGACCTTGTGAACAATTAATTGTGTC; *spr-5*, GTAAACTTCGAAGAG-CACGGAG and CCGCCACTCCATTCTCC; *hop-1*, GGACTAGTCGTAT-TAGCCAACAGCAT and CCGGCTCGAGAGCTGAAATTTGTC; *lin-12*, TCAGGAAAACGGGAACCATT and AATCGGCGTCTTCCATCTT; *efl-1*, ACATGGAGCTTCAAAAAGCG and CAATTCCTTCGAGAACATTTCG. The T7 promoter sequence used was TAATACGACTCACTATAGGGA. All other primers were as previously described (Fay et al., 2002).

## Results

### *lin-35/Rb* and *spr-1/slr-10* are genetically redundant

Using a previously described genetic screen to identify proteins that perform overlapping functions with LIN-35 (Fay et

al., 2002), we isolated a single allele (*fd6*) defining a locus originally designated as *slr-10* (for *synthetic* with *lin-35/Rb*; hereafter referred to as *spr-1*). Briefly, *lin-35(n745)* homozygous animals that carry an extrachromosomal array (*kuEx119*) expressing wild-type *lin-35* along with a GFP reporter were subjected to chemical mutagenesis. Following an F2 clonal screen, strains harboring synthetic mutations were identified based on the expression of visible phenotypes in animals that failed to inherit the array. Whereas both *lin-35* and *spr-1(fd6)* single mutants were largely indistinguishable from wild type, *lin-35; spr-1* double mutants were smaller and slower growing and had an abnormally clear or mottled appearance (Figs. 1A, B; data not shown). Also, as described below, *lin-35; spr-1* mutants showed defects in vulval morphogenesis, somatic gonad development, and fertility.

### *fd6* defines a mutation in *spr-1*, the *C. elegans* ortholog of human CoREST

*fd6* was mapped to a small region on the right arm of LGV using classical genetic and SNP mapping techniques (see Materials and methods; Fay, 2006). Two overlapping cosmids in the region, D1014 and F20D6, rescued the synthetic defects

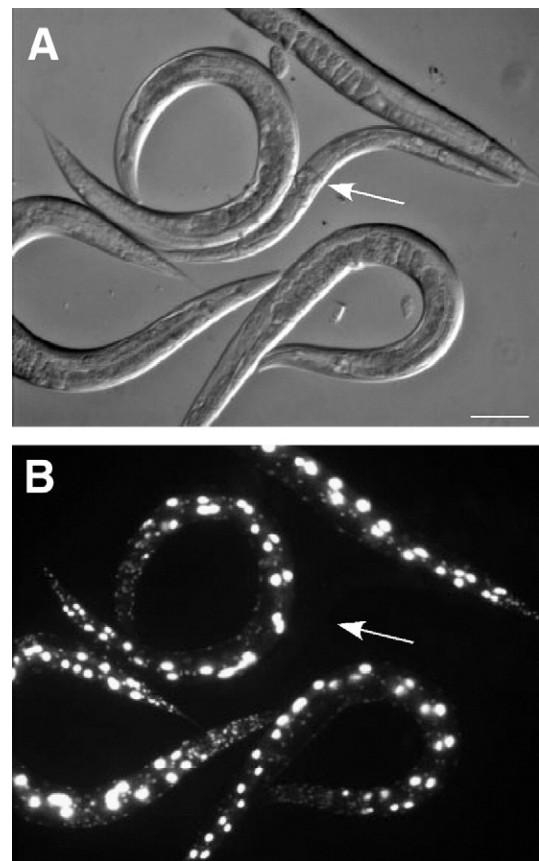


Fig. 1. A synthetic genetic interaction between *lin-35(n745)* and *spr-1(fd6)*. DIC (A) and corresponding GFP fluorescence (B) images. White arrow indicates the position of the affected *lin-35; spr-1* mutant that has failed to segregate the *kuEx119* rescuing array. Scale in panel A, 100  $\mu$ m for panels A, B.

of *lin-35*; *spr-1* animals completely. RNAi of genes contained on these cosmids in the *lin-35* mutant background led to the identification of a single clone (corresponding to D1014.8/*spr-1*) that closely phenocopied the effects of the *fd6* mutation (also see below). Sequence analysis of the *spr-1* coding region in the *fd6* mutant background revealed a C to T transition at nucleotide position 1375 of the *spr-1* cDNA. This mutation produces a premature translational stop codon following amino acid 458 of the 558-amino-acid protein. Based on these data, along with the observed synthetic genetic interactions of other *spr-1* alleles with *lin-35* (see below) and the failure of a previously isolated allele of *spr-1* to complement *fd6* (see Materials and methods) we conclude that *spr-1* is the relevant locus defined by *fd6*.

*spr-1* encodes an ortholog of the human CoREST protein (Jarriault and Greenwald, 2002), which acts within a larger complex that includes the REST/NRSF tumor suppressor (Andres et al., 1999; Westbrook et al., 2005). The REST/CoREST complex is thought to represses the transcription of genes through the recruitment of histone deacetylases (Humphrey et al., 2001; You et al., 2001) and demethylases (Lee et al., 2005) to specific target sites. The *fd6* mutation leads to a C-terminal truncation of SPR-1 just preceding the second of two conserved SANT domains. SANT domains are found in a number of chromatin remodeling enzymes and have been shown to function in chromatin binding through interactions with histone tails (Boyer et al., 2002).

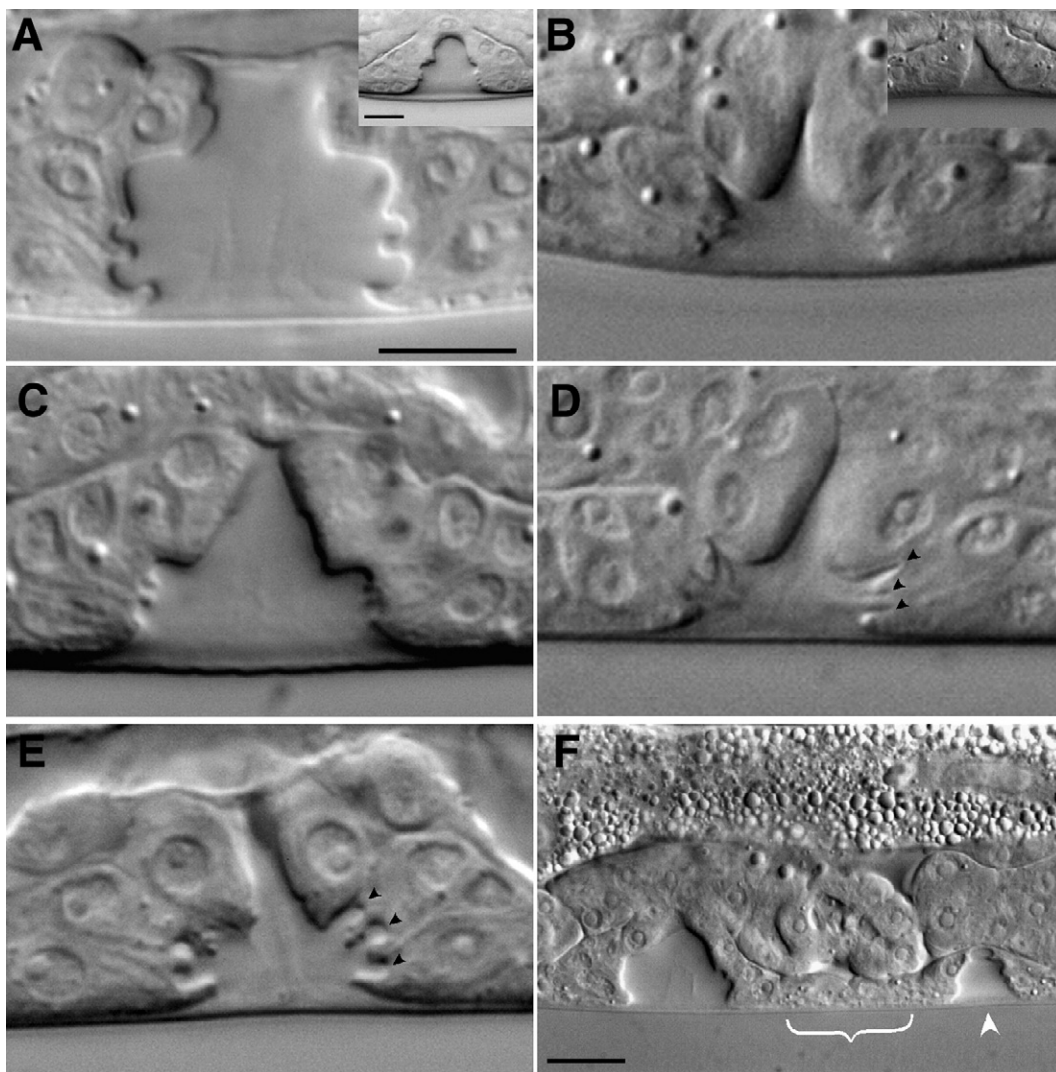


Fig. 2. *lin-35*; *spr-1* mutants have defects in vulval morphogenesis. DIC images of mid-L4-stage wild-type (A), *lin-35*(n745); *spr-1*(*fd6*) double mutant (B, C), *lin-35*; *spr-1*(RNAi) (D), *sqv-2*(n2826) (E), and *rib-2*(*gk318*) (F) hermaphrodite animals. Note the reduction in the area of the vulval lumen in the double mutants (B–D) and *sqv-2* (E) as compared with wild type (A). Panels B and C show the range of Sqv phenotypes (most to least severe) displayed by the double mutants. Insets in panels A and B show vulval development in wild-type and *lin-35*; *spr-1* animals at the early L4 stage. Note that the vulval lumen is compressed in double mutants relative to wild type at this stage. Black arrowheads (D, E) demarcate the luminal processes formed by the vulval toroids. Note the increased compression of luminal processes in the double mutants (B–D) versus the wild-type (A) and *sqv-2* (E) animals. *rib-2* mutants (F) do not display a Sqv phenotype but do show a low penetrance of vulval induction defects. The animal in panel F has an abnormal induction of the P8p.a lineage (white arrowhead) as well as an apparent under-induction of the P7.p lineage (white bracket). Scale bar in panel A, 10  $\mu$ m for panels A–E; in panel A inset, 10  $\mu$ m for panels A, B insets; in panel F, 10  $\mu$ m.

Given that the original alleles of *spr-1* were identified on the basis of their ability to suppress the egg-laying defective (Egl) phenotype of *sel-12* presenilin mutants (Jarriault and Greenwald, 2002), we tested *spr-1(fd6)* for this capacity and found that it suppressed the Egl phenotype of 10/10 *sel-12* (*ar171*) animals, indicating that *spr-1(fd6)* can function in its canonical role as a *sel-12* suppressor. In contrast, 34/34 *lin-35; sel-12* mutants were incapable of laying eggs, indicating that *lin-35* does not share this specific suppressive function with *spr-1*.

#### *lin-35; spr-1* double mutants display defects in vulval morphogenesis

The *C. elegans* hermaphrodite egg-laying and mating organ, the vulva, is derived from three epithelial precursor cells, which undergo a well-defined series of cell divisions along with morphogenetic events that include migrations, cell shape changes, and cell fusions (Sternberg, 2005). During the mid-L4-stage, the vulva acquires a stereotypical “Christmas tree” morphology at which time it is comprised of seven vertically stacked multinucleate toroid (ring-shaped) cells that contain a large central lumen (Figs. 2A, 3I). A number of mutations have been characterized that specifically affect the morphogenetic steps of vulval development including eight loci that result in a partially collapsed or “squashed” vulval lumen (the Sqv phenotype) at the L4 stage (Fig. 2E; Herman et al., 1999; Sternberg, 2005). Although morphogenesis is severely defective, these *sqv* mutants display a wild-type pattern of vulval cell divisions along with normal hallmarks of cell differentiation (Herman et al., 1999).

We found that most *lin-35; spr-1* double mutants exhibited a phenotype that was similar to that previously reported for the *sqv* mutants. Namely, the vulval lumen of *lin-35; spr-1* mutants was substantially compressed at the mid-L4 stage relative to wild type or the large majority of *lin-35* and *spr-1* single mutants (Figs. 2B, C; Table 1; data not shown). This defect in vulval morphogenesis was also observed in *lin-35; spr-1(RNAi)* and *spr-1; lin-35(RNAi)* animals (Fig. 2D; Table 1) including

(in the latter case) multiple independently isolated alleles of *spr-1* (Table 1). The Sqv-like phenotype was also manifest in double mutants at time points preceding the mid-L4 stage (Figs. 2A, B insets, 3C, 4I), similar to previously described *sqv* mutants (Herman et al., 1999). This indicates that underlying defect in *lin-35; spr-1* double mutants somehow impinges on the ability of the vulval cells to undergo normal ingression.

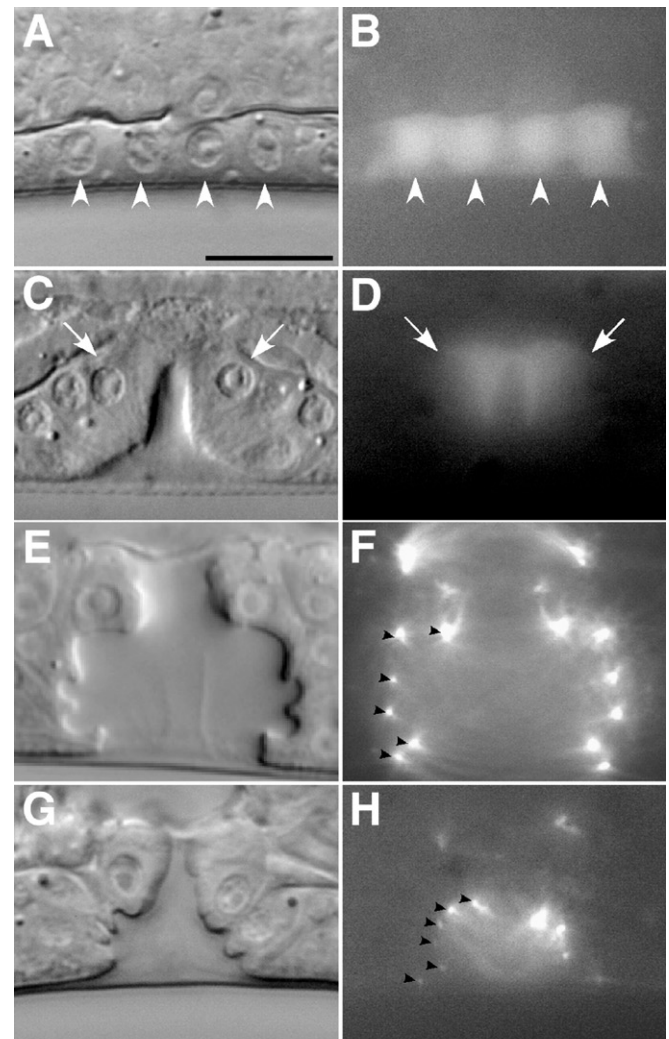


Fig. 3. *lin-35; spr-1* mutants undergo normal vulval cell divisions, differentiation patterns, and cell fusion events. DIC (A, C, E, G) and corresponding GFP fluorescence (B, D, F, H) images of wild-type (E, F) and *lin-35; spr-1(fd6)* (A–D, G, H) developing vulvae. Panel I shows the vulval cell lineage during the L3 stage and a schematic of vulval morphology at the mid-L4 stage in wild-type animals. The fates of nuclei within the L3 lineage and the L4 vulva are indicated by color; wild-type *egl-17::GFP* expression is indicated by the green line circumscribing cells in the lineage diagram (A, B) L3- and (C, D) L4-stage *lin-35; spr-1* mutants showing normal expression of *egl-17::GFP* in L3-stage P6.p derivatives (A, B; white arrowheads) and in the L4-stage N-cells of P5.p and P7.p (C, D; white arrows; the T-cells are not visible in this focal plane). (E–H) *ajm-1::GFP*, which marks the adherens junctions between the vulval toroids in wild-type (E, F) and *lin-35; spr-1* L4 animals (G, H). Black arrowheads indicate the GFP-marked junctions between the vulval toroids. Although expression of this marker is fainter in the *lin-35; spr-1* mutants (most likely due to the silencing effect of *lin-35* mutations on transgenic arrays; Hsieh et al., 1999), seven toroids can reproducibly be identified in vulvae from both animals. Scale bar in panel A, 10  $\mu$ m, for panels A–H.

Table 1  
Vulval and germline phenotypes

Genotype	Sqv (%)	Oocytes/arm
N2	0 (n=31)	7.0 ( $\pm$ 1.4) (range, 4–10) (n=52)
<i>lin-35</i> (n745)	11 (n=27)	6.7 ( $\pm$ 1.7) (range, 4–12) (n=27)
<i>spr-1</i> ( <i>fd6</i> )	3 (n=30)	7.8 ( $\pm$ 1.9) (range, 5–11) (n=28)
<i>spr-1</i> ( <i>ar205</i> )	0 (n=26)	ND
<i>spr-1</i> ( <i>ar200</i> )	7 (n=28)	ND
<i>lin-35; spr-1</i> ( <i>fd6</i> )	63 (n=88)	2.9 ( $\pm$ 1.2) (range, 1–5) (n=28)
<i>lin-35; spr-1</i> ( <i>ar205</i> )	53 (n=30)	2.6 ( $\pm$ 0.9) (range, 1–4) (n=38)
<i>spr-1</i> ( <i>fd6</i> ); <i>lin-35</i> ( <i>RNAi</i> )	48 (n=21)	ND
<i>spr-1</i> ( <i>ar200</i> ); <i>lin-35</i> ( <i>RNAi</i> )	26 (n=19)	ND
<i>spr-1</i> ( <i>ar205</i> ); <i>lin-35</i> ( <i>RNAi</i> )	27 (n=22)	ND
<i>lin-35; spr-1</i> ( <i>RNAi</i> )	64 (n=36)	4.5 ( $\pm$ 1.7) (n=36)
<i>spr-4</i> ( <i>RNAi</i> )	8 (n=35)	ND
<i>lin-35; spr-4</i> ( <i>RNAi</i> )	53 (n=15)	ND
<i>spr-5</i> ( <i>RNAi</i> )	10 (n=20)	ND
<i>lin-35; spr-5</i> ( <i>RNAi</i> )	67 (n=24)	ND
<i>lin-35; spr-1</i> ( <i>fd6</i> ); <i>lin-12</i> ( <i>RNAi</i> )	54 (n=26)	2.5 ( $\pm$ 1.0) (range, 1–5) (n=29)
<i>lin-35; spr-1</i> ( <i>fd6</i> ); <i>hop-1</i> ( <i>RNAi</i> )	77 (n=22)	2.9 ( $\pm$ 1.0) (range, 1–5) (n=30)
<i>lin-12</i> ( <i>RNAi</i> )	7 (n=27)	6.4 ( $\pm$ 0.9) (range, 5–8) (n=27)
<i>hop-1</i> ( <i>RNAi</i> )	0 (n=21)	6.5 ( $\pm$ 1.0) (range, 5–9) (n=21)

All RNAi experiments were carried out using injection methods. *n* values for oocyte counts were based on individual gonad arms.

Our analysis of vulval development in the double mutants based on the cell lineage did not reveal any obvious defects. Cells divisions occurred in their normal characteristic planes and with the appropriate relative timing to consistently produce 22 nuclei (data not shown). To more thoroughly assess vulval cell fate specification and differentiation in *lin-35; spr-1* animals, we examined expression of the *egl-17::GFP* marker in the double mutants (gift of M. Stern). In wild-type animals, *egl-17::GFP* is initially expressed in dividing vulval cells that are derivatives of P6.p. Following the terminal divisions, this expression shifts to the N and T lineages of P5.p and P7.p (Fig. 3I; *Burdine et al., 1998*). We found that wild-type and *lin-35; spr-1* animals showed identical patterns of *egl-17::GFP* expression, further indicating that vulval cells in the double mutants adopt their correct fates (Figs. 3A–D; data not shown). We also assessed the ability of vulval cells in *lin-35; spr-1* animals to form multinucleate toroid-shaped cells using the adherens junction marker *ajm-1::GFP* (gift of J. Hardin; *Mohler et al., 1998*). Wild-type L4 animals contain seven toroids and thus six easily identifiable (GFP-marked) foci located at the junction of each toroid (n=14; Figs. 3E, F). Similarly, *lin-35; spr-1* double mutants contained an average of  $5.9 \pm 0.3$  (n=10) GFP-positive foci at this same stage (Figs. 3G, H). Taken together, these data strongly indicate that there is a lack of vulval cell lineage, differentiation, and fusion defects in *lin-35; spr-1* double mutants and imply that the observed morphogenesis defects are due to other causes.

Our finding that vulval cell patterning and cell-fate assignments appear to be normal in the double mutants is similar to previous findings with other *sqv* mutants (*Herman et al., 1999*). We did note several qualitative differences, however, between the vulval morphologies of *lin-35; spr-1* mutants and previously described *sqv* mutants. Specifically, compression of the luminal

processes that delineate the toroid rings was typically more severe in *lin-35; spr-1* animals (Figs. 2B–E). In addition, the vulval phenotype of double mutants displayed more variability than was seen for most *sqv* mutants (Figs. 2B–D, 3G; data not shown).

*The synthetic Sqv phenotype of lin-35; spr-1 mutants does not result from gross defects in chondroitin biosynthesis or localization*

Investigation of the eight previously characterized *sqv* genes has placed them in a coherent pathway involved in the biosynthesis of the glycosaminoglycans (GAGs) heparan sulfate and chondroitin (*Herman and Horvitz, 1999; Bulik et al., 2000; Hwang and Horvitz, 2002a,b; Hwang et al., 2003a*). Furthermore, the identification of a glycosyltransferase (SQV-5) that is specific for the biosynthesis of chondroitin has implicated chondroitin deficiencies as the underlying cause of the Sqv phenotype (*Hwang et al., 2003b*). In support of this, we found that *rib-2*, which encodes an enzyme required specifically for the initiation and elongation of heparan sulfate (*Kitagawa et al., 2001; Morio et al., 2003*), was not required for the formation of a normal vulval lumen (n=40; Fig. 2F). Interestingly, we did observe a low frequency (14%, n=29) of vulval induction defects in *rib-2(gk318)* mutants (Fig. 2F), suggesting that as in other systems, heparan sulfate may modulate paracrine signaling through the conjugation of peptide growth factors in *C. elegans* (*Powell et al., 2004; Iwamoto and Mekada, 2006*).

In order to test whether chondroitin biosynthesis is impaired in *lin-35; spr-1* double mutants, lysates were prepared from synchronized wild-type, *lin-35*, and *spr-1* single-mutant animals as well as *lin-35* mutants subjected to *spr-1* RNAi feeding. Following treatment with chondroitinase ABC, samples were separated by electrophoresis, transferred to a membrane, and probed with a mAb directed against the remaining stub oligosaccharides on chondroitin proteoglycans (*Olson et al., 2006*). Although there may have been a slight reduction in the total levels of chondroitin proteoglycans in *lin-35* single mutants versus wild type, the levels in *lin-35; spr-1* (*RNAi*) double mutants were equivalent to those in *lin-35* single mutants (based on two independent experiments; Fig. 5A and data not shown). These results indicate that *lin-35* and *spr-1* do not function redundantly to promote chondroitin biosynthesis, and that in contrast to the *sqv* mutants, the Sqv phenotype in double mutants is not correlated with a strong reduction in chondroitin biosynthesis.

To determine whether *lin-35; spr-1* mutants might exhibit localized changes in chondroitin levels, we carried out immunocytochemistry to assay chondroitin expression in whole animals. Although this staining procedure showed some inherent variability within controlled sample sets, we did observe clear vulval staining in the majority of L4-stage wild-type (24/27) and *lin-35; spr-1* (17/24) double mutants. Furthermore, staining levels of the two genotypes were observed to be roughly equivalent (Figs. 5B–E; data not shown). As a control, no staining was observed in *sqv-2(n2826)* mutants, which are defective at chondroitin biosynthesis (Figs.

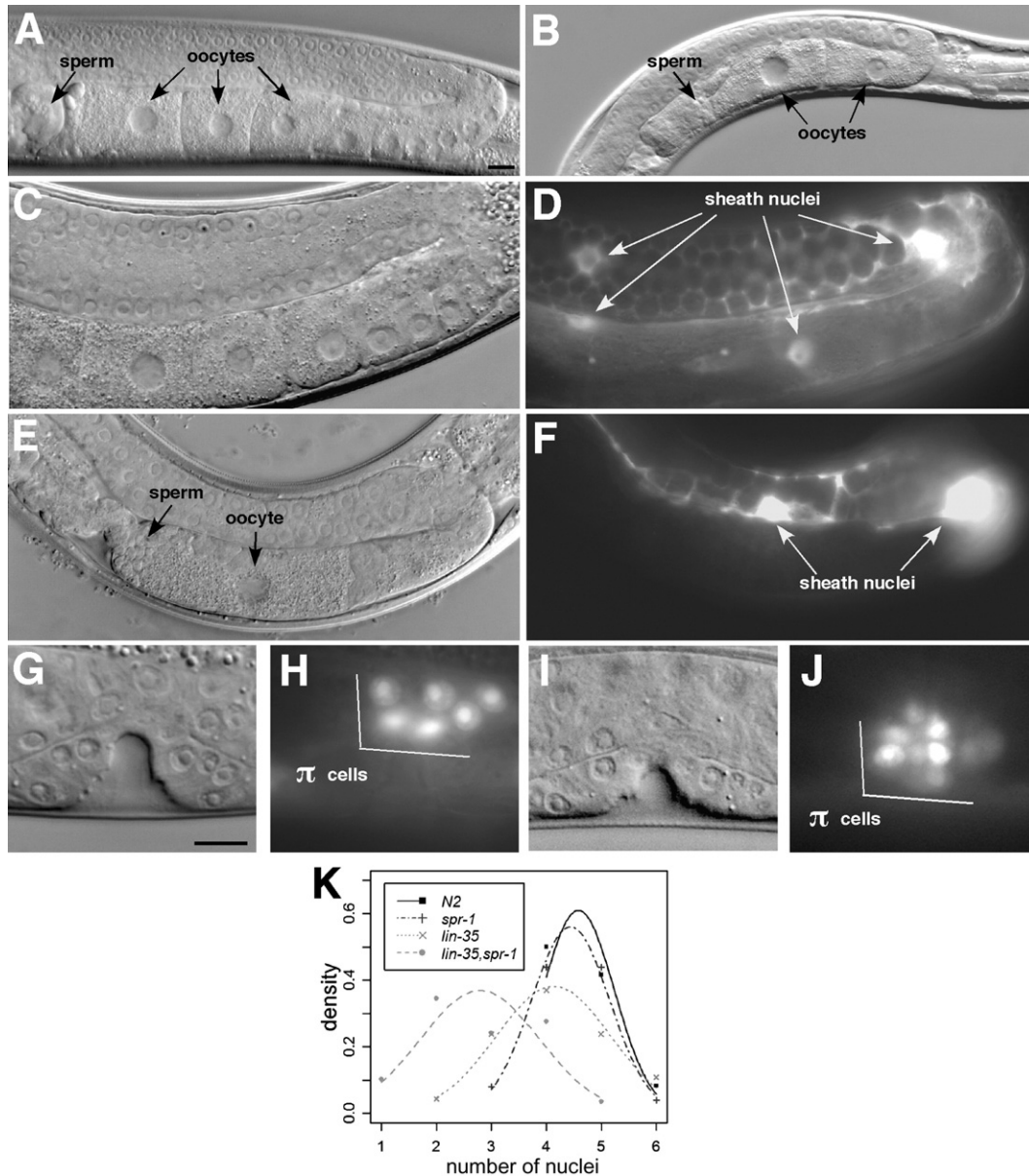


Fig. 4. *lin-35; spr-1* mutants show defects in gonad morphology and somatic cell positioning. DIC images of wild-type (A) and *lin-35; spr-1(fd6)* mutant (B) adult gonads. Note reduction in the size and number of oocytes in the double mutant. DIC (C, E, G, I) and corresponding GFP fluorescence (D, F, H, J) images of wild-type (C, D, G, H) and *lin-35; spr-1* (E, F, I, J) adult (C–F) or L4-stage (G–J) animals. Panels C–F show gonads in animals that express the *lim-7::GFP* marker for sheath cells. Note the reduction in expression of the marker in the proximal half of the gonad arm in the *lin-35; spr-1* mutant. Panels G–J show animals that express the *cog-2::GFP* marker for uterine  $\pi$  cells. Whereas the majority of wild-type animals contained six lateral  $\pi$  cells per side (G, H), *lin-35; spr-1* mutants typically showed an asymmetry in  $\pi$  cell distribution (I, J). This difference was highly significant according to a two-sample *t* test ( $p \ll 0.001$ ). (K) Distribution of proximal sheath cell nuclei in wild-type, *lin-35; spr-1*, and *lin-35; spr-1* animals. Dots represent experimental data; curves represent corresponding best-fit normal-distribution density functions. Wild-type animals contained an average of 4.6 ( $n=24$ ; range, 4–6) sheath cell nuclei within the proximal half of their gonad arms, whereas *lin-35; spr-1* double mutants contained an average of 3.0 ( $n=29$ ; range, 1–5) nuclei in this region. This difference was very significant according to a two-sample *t* test ( $p \ll 0.001$ ). Scale bar in panel A, 10  $\mu$ m, for panels A–F; in panel G, 10  $\mu$ m, for panels G–J.

5F, G). Based on these findings, along with several qualitative differences in the outward appearance of the vulval phenotype (see above), we conclude that unlike previously identified *sqv* mutants, the synthetic *Sqv* phenotype of *lin-35; spr-1* double mutants is not attributable to either substantive global or local alterations in chondroitin biosynthesis or distribution. This conclusion is further supported by our observation that simultaneous loss of *lin-35*, *spr-1* and either *sqv-2* or *sqv-7* leads to vulval phenotypes that are qualitatively additive and

also typically more severe than either *lin-35; spr-1* or the *sqv* mutants alone (data not shown).

*lin-35; spr-1* double mutants display fertility and germline defects

*lin-35; spr-1* animals that failed to inherit the rescuing array displayed a substantially reduced brood size compared with wild type and single mutants (Table 2). This effect on brood size

was greatly exacerbated in subsequent generations of double-mutant animals derived from parents that lacked the *kuEx119* extrachromosomal array (Table 2). Similar fertility defects were also observed in *lin-35; spr-1(ar205)* mutant animals, further demonstrating that other alleles of *spr-1* can synergize with *lin-35* loss of function (LOF; Table 2). Consistent with the observed

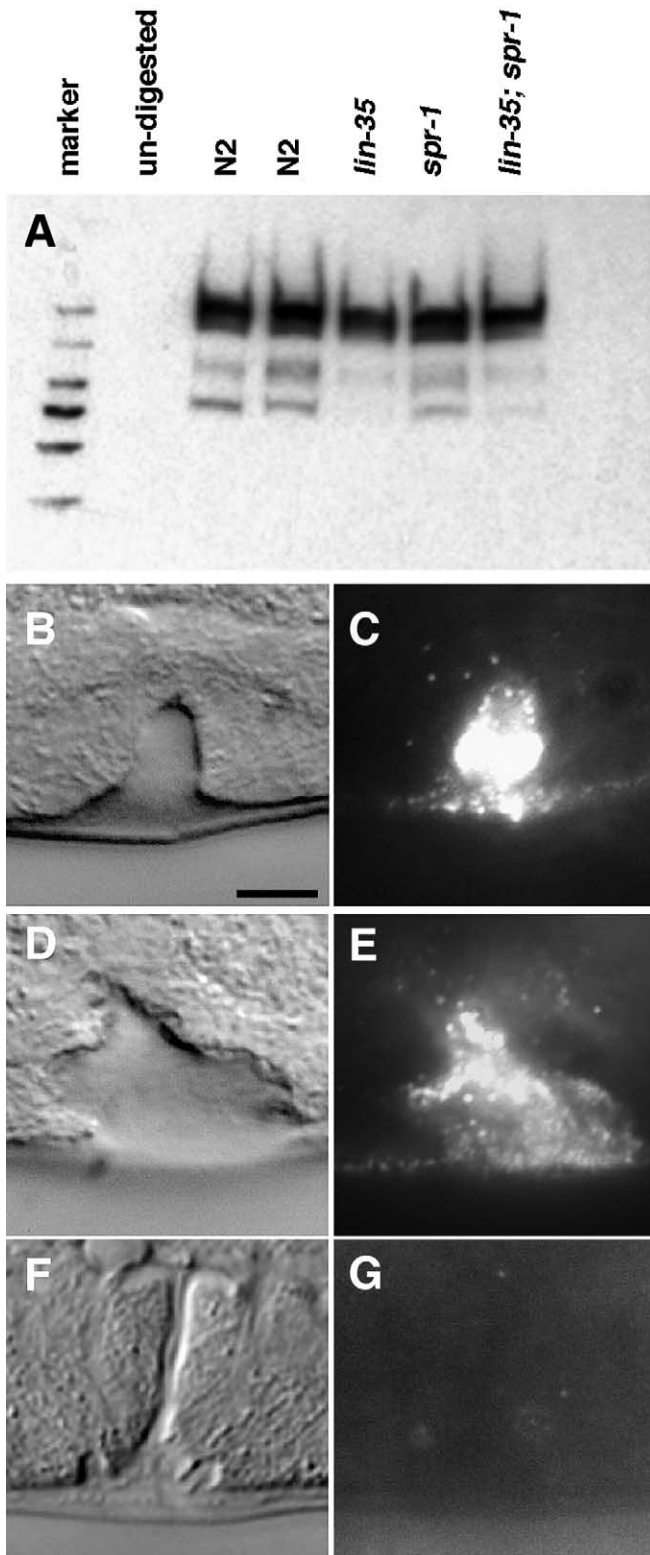
Table 2

Brood size analysis

Genotype	Brood size	Sterility (%)
N2 <sup>a</sup>	264 (±18) (n=50)	0 (n=50)
<i>lin-35(n745)</i> <sup>a</sup>	98 (±43) (n=10)	3 (n=100)
<i>spr-1(fd6)</i>	215 (±41) (n=20)	0 (n=20)
<i>lin-35; spr-1(fd6)</i>	20 (±18) (n=43)	10 (n=48)
<i>lin-35; spr-1(fd6)</i> (Mat <sup>-</sup> ) <sup>b</sup>	5 (±3) (n=10)	86 (n=70)
<i>lin-35; spr-1(ar205)</i>	19 (±13) (n=15)	4 (n=25)
<i>lin-35; spr-1(ar205)</i> (Mat <sup>-</sup> ) <sup>b</sup>	12 (±13) (n=13)	57 (n=30)

<sup>a</sup> Brood size results taken from Fay et al., 2002.

<sup>b</sup> Mat<sup>-</sup> indicates that the double-mutant animals were derived from parents that lacked the *kuEx119* extrachromosomal array, which may contribute maternal *lin-35*.



fertility defects, DIC and DAPI staining revealed that double mutants have substantially smaller gonad arms relative to those of wild type or single mutants and contain fewer germ cells (the Glp phenotype) at all stages and fewer oocytes in adults (Figs. 4A, B, 6A–D; Table 1; data not shown). The gonadal and germline defects observed in the double mutants were robustly rescued by expression of either *lin-35* or *spr-1* via a repetitive extrachromosomal array (Fig. 1; data not shown). Given that such arrays are typically silenced in the germline, this suggests that the underlying defects may be due to a somatic requirement for these genes.

The impaired fertility and diminutive gonads of *lin-35; spr-1* double mutants are similar to previous findings for *xnp-1 lin-35* double mutants (Bender et al., 2004). In the case of *xnp-1 lin-35* animals, this defect could be attributed to an absence or significant reduction in the number of gonadal sheath cells, which are required for proper expansion of the germline stem cell population during larval development (McCarter et al., 1997; Killian and Hubbard, 2005). To examine the status of sheath cells in double mutants, we used the *lim-7::GFP* reporter, which is expressed consistently in the cytoplasm (and more variably in the nuclei) of 8 of the 10 sheath cell pairs (1–4) that encapsulate each gonad arm (Hall et al., 1999). We observed an average of 7.0 sheath cell nuclei (n=24; range, 6–8) per gonad arm in wild-type animals (Figs. 4C, D). Similarly, *lin-35; spr-1* double mutants had 6.5 sheath cell nuclei (n=29; range, 5–8) per gonad arm (Figs. 4E, F). From this we conclude that there is not a gross deficiency in the number of sheath cell nuclei in *lin-35; spr-1* double mutants, although it is possible that these cells are nevertheless defective in their ability to promote germ cell proliferation. We note that although sheath cell number did not differ appreciably from that of wild type, we

Fig. 5. Analysis of chondroitin expression in wild type and mutants. (A) Western blot indicating levels of chondroitin in wild-type, *lin-35* single-mutant, and *lin-35; spr-1(RNAi)* animals. The multiple bands indicate several species of chondroitin proteoglycan core proteins. DIC (B, D, F) and fluorescence (C, E, G) images of wild-type (B, C), *lin-35; spr-1* (D, E), and *sqv-2(n2826)* mutants early- or mid-L4 vulvae stained with a mAb specific for the chondroitin stub epitope. The majority of both wild-type and *lin-35; spr-1* L4 animals showed similar vulval-specific staining patterns that were never observed in *sqv-2* (*n2826*) mutants, which cannot synthesize chondroitin. Also see Results. Scale bar in panel B, 10 μm, for panels B–G.

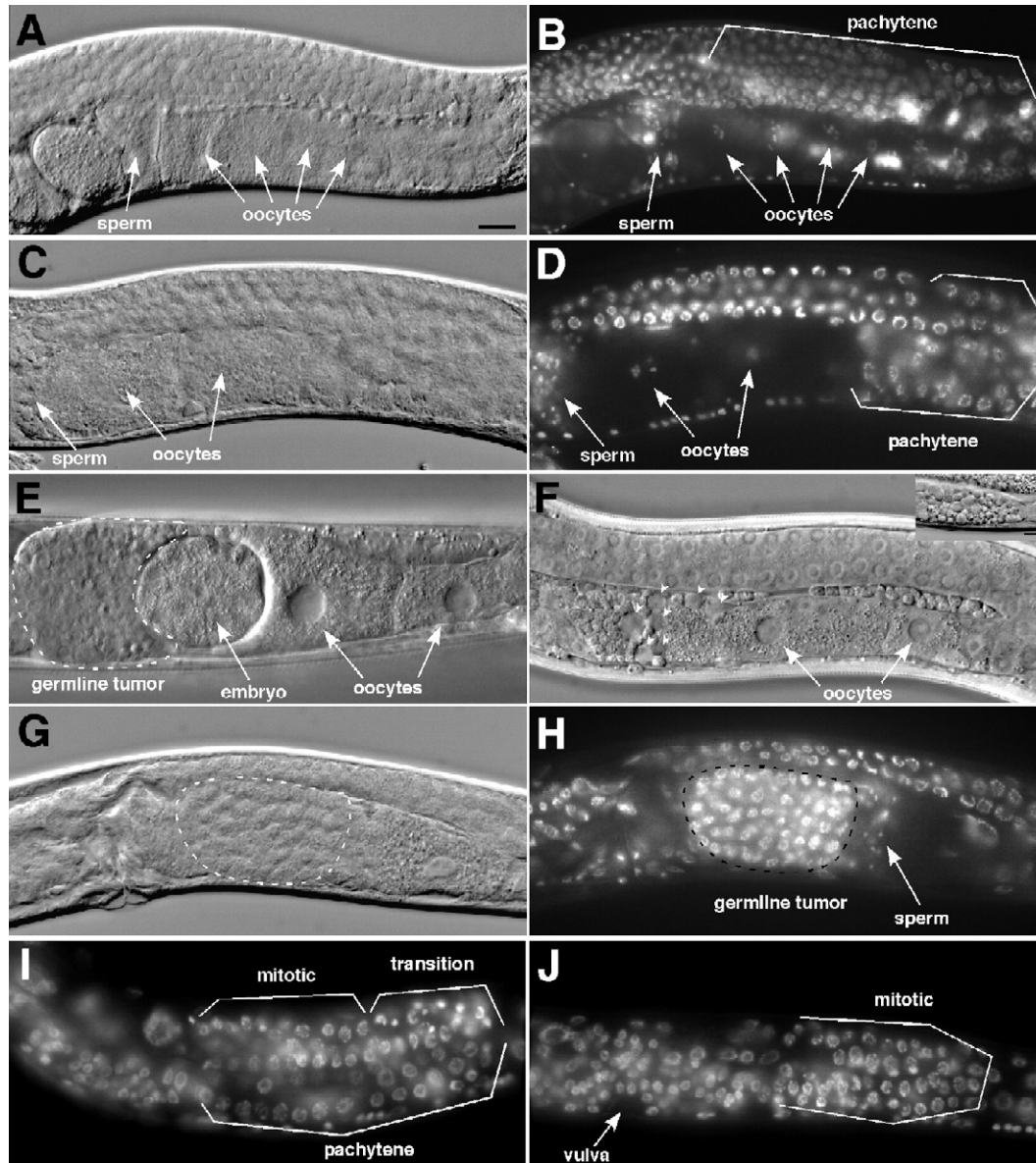


Fig. 6. Germline defects in *lin-35; spr-1* and *lin-35; spr-1; hop-1* mutants. DIC (A, C) and corresponding DAPI fluorescence (B, D) images of wild-type (A, B) and *lin-35; spr-1(fid6)* (C, D) adults. Note the reduction in germ cell numbers and oocytes as well as the extended pachytene meiotic region present in *lin-35; spr-1* double mutants versus wild type (B, D). Proximal germline tumor (E) and residual bodies from spermatocytes (white arrowheads; F) in the gonads of *lin-35; spr-1; hop-1(RNAi)* adult animals. Inset in panel F shows the morphology of a late-stage L4/early adult animal containing spermatocytes, residual bodies, and spermatids for reference. DIC (G) and corresponding DAPI fluorescence (H) images of *lin-35; spr-1; hop-1(RNAi)* animals. The tumor nuclei are densely packed and have a morphology characteristic of mitotically dividing cells. DAPI staining of (I) *lin-35; lin-12(RNAi)* and (J) *lin-35; spr-1; lin-12(RNAi)* mid-L4-stage animals. Note the absence of transition and pachytene meiotic nuclei in the triple mutants. Scale bar in panel A, 10  $\mu$ m, for panels A–J, in panel F inset, 10  $\mu$ m.

did observe a strong shift in the positioning of the sheath cells in *lin-35; spr-1* animals toward the distal half of the gonad arm (Figs. 4E, F, K), a phenomenon that could be a secondary consequence of germline proliferation defects.

We also examined  $\pi$  cells of the ventral uterine lineage using the *cog-2::GFP* reporter (Hanna-Rose and Han, 1999). We observed an average of 12  $\pi$  cells in both wild-type ( $n=24$ ; range, 11–13) and *lin-35; spr-1(RNAi)* ( $n=24$ ; range, 10–13) animals, indicating that  $\pi$  cells are also correctly specified in the double mutant. However, whereas 79% of wild-type animals consistently had 6  $\pi$  cells per lateral side at the mid-L4 stage ( $n=24$ ), only 25% ( $n=24$ ) of *lin-35; spr-1(RNAi)* animals

displayed an equal lateral distribution of these cells (Figs. 4G–J). In contrast, single mutants did not display  $\pi$  cell distribution defects (data not shown). These data suggest that although *lin-35* and *spr-1* are not required for cell-type specification or differentiation per se, they may redundantly regulate subtle aspects of somatic gonad development such as organization, morphology, and function.

#### *spr-1* is synthetic with other Class B SynMuv genes

To determine whether the vulval and germline defects observed in *lin-35; spr-1* mutants could be phenocopied by

Table 3  
*spr-1(fld6)* interactions with synthetic multivulval (SynMuv) genes

RNAi <sup>a</sup>	SynMuv class	Sqv (%)
Vector <sup>b</sup>	–	0 (n=22)
H <sub>2</sub> O <sup>c</sup>	–	3 (n=30)
<i>lin-35</i>	B	31 (n=54)
<i>lin-36</i>	B	0 (n=13)
<i>lin-37</i>	B	45 (n=20)
<i>efl-1</i>	B	17 (n=42) <sup>d</sup>
<i>lin-15a</i>	A	9 (n=43) <sup>e</sup>
<i>trr-1</i> <sup>f</sup>	C	0 (n=18)

<sup>a</sup> RNAi was carried out using standard feeding methods (Ahringer, 2005) with the exception of *efl-1*, which was carried out using injection methods. As a control, all of the clones tested were observed to induce a highly penetrant multivulval phenotype in the appropriate genetic backgrounds (data not shown).

<sup>b</sup> pPD129.36 was used as the control empty vector for the feeding experiments.

<sup>c</sup> Injection of H<sub>2</sub>O is the control for *efl-1* RNAi.

<sup>d</sup> *p*-value based on proportion tests (relative to H<sub>2</sub>O injection)= $2.0 \times 10^{-4}$ .

<sup>e</sup> *p*-value based on proportion tests (relative to H<sub>2</sub>O injection)=0.04.

<sup>f</sup> *trr-1*(RNAi) caused a low-percentage multivulval phenotype in the *spr-1* mutant background (data not shown).

reducing the activities of other SynMuv genes (see Introduction), we tested several class B as well as one class A and one class C genes for genetic interactions with *spr-1* (Table 3; reviewed by Sternberg, 2005; Fay and Han, 2000). Of the class B genes tested, *lin-37* along with the E2F ortholog *efl-1* produced strong and moderate effects, respectively. In contrast, *lin-36* failed to show an interaction, indicating that some, but not all, class B genes function with *lin-35* in its redundant role with *spr-1*. Furthermore, the class A (*lin-15a*) and class C (*trr-1*) genes showed only weak or no effects, similar to previous *slr* mutants studied (Fay et al., 2002, 2003, 2004; Bender et al., 2004).

We also note that inactivation of several other components of the *C. elegans* CoREST complex in the *lin-35* mutant background led to similar synthetic defects as those observed with *spr-1*. These included *spr-4*, which encodes a C2H2-type finger protein (Lakowski et al., 2003), and *spr-5*, a putative histone demethylase (Table 1; Eimer et al., 2002; Jarriault and Greenwald, 2002). Taken together, these results support the model that both *lin-35* and *spr-1* carry out their redundant functions within the context of multisubunit transcriptional regulatory complexes.

#### The *lin-35; spr-1* phenotype is not likely to be attributable to LIN-12/Notch hypersignaling

As described above, *spr-1* was originally identified for its ability to suppress the Egl phenotype of *sel-12* mutants (Jarriault and Greenwald, 2002), and *sel-12* is itself a suppressor of gain-of-function (GOF) mutations in *lin-12*/Notch (Levitan and Greenwald, 1995). *sel-12* encodes a presenilin-like protease that is required for the (site 3) cleavage and signaling capacity of Notch receptors (Greenwald, 2005). A second presenilin gene in *C. elegans*, *hop-1*, functions redundantly with *sel-12*, as *hop-1; sel-12* double mutants are synthetically lethal (Li and Greenwald, 1997; Westlund et al., 1999). It has been suggested that

the *C. elegans* CoREST complex may act directly on the *hop-1* locus to mediate transcriptional repression, as *hop-1* mRNA is upregulated in several CoREST complex mutant backgrounds (Eimer et al., 2002; Lakowski et al., 2003). Thus, it was possible that the synthetic phenotype of *lin-35; spr-1* mutants is due, at least in part, to an increase in *hop-1* abundance and, by extension, LIN-12/Notch signaling activity.

To test this model, we inactivated *lin-12* and *hop-1* in *lin-35; spr-1* mutants using RNAi injection methods and scored for suppression of the synthetic Sqv and germline defects. The efficacy of these RNAi treatments was first verified by showing that *lin-12*(RNAi) induced a highly penetrant Egl phenotype in wild-type animals and that *hop-1*(RNAi) led to synthetic lethality in the *sel-12* mutant background (data not shown; Sundaram and Greenwald, 1993; Li and Greenwald, 1997; Westlund et al., 1999). We found that neither treatment was capable of mitigating either the vulval or germline defects of the double mutants (Table 1). These results indicate that increased levels of HOP-1 activity or LIN-12 signaling are unlikely to be a cause of the double mutant phenotype. Consistent with this, other phenotypes associated with *lin-12* hypermorphic alleles, such as the ectopic induction of secondary vulval cell fates or loss of the gonadal anchor cell, were not observed in the double mutants (data not shown; Sternberg, 2005; Greenwald, 2005).

#### *lin-35; spr-1* double-mutant germlines are hypersensitive to reductions in *lin-12*/Notch signaling

Although we failed to detect any suppressive effects of *hop-1* or *lin-12* RNAi on the vulval and germline defects of *lin-35; spr-1* mutants, we did observe proximal germline tumors (the Pro phenotype) in 21 and 24% of individual gonad arms from *lin-35; spr-1; hop-1*(RNAi) and *lin-35; spr-1; lin-12*(RNAi) animals, respectively (referred to as triple mutants; Figs. 6E, G, H; Table 4). In contrast, *lin-35; spr-1* double mutants as well as all other possible binary combinations of double mutants

Table 4  
Proximal germline proliferation (Pro) phenotypes

Genotype	Pro (%) <sup>a</sup>	Adults containing residual bodies (%) <sup>a</sup>
N2	0 (n=69)	6 (n=69)
<i>lin-35; spr-1</i>	2 (n=98)	11 (n=37)
<i>hop-1; spr-1</i> <sup>b</sup>	2 (n=126)	13 (n=31)
<i>lin-35; hop-1</i> (RNAi)	0 (n=58)	ND
<i>lin-35; spr-1; hop-1</i> (RNAi)	21 (n=154)	44 (n=52)
<i>lin-35; sel-12</i> <sup>c</sup>	0 (n=40)	ND
<i>lin-35; sel-12; spr-1</i> <sup>b,c</sup>	10 (n=61)	23 (n=61)
<i>spr-1; lin-12</i> (RNAi) <sup>d</sup>	0 (n=37)	11 (n=37)
<i>lin-35; lin-12</i> (RNAi)	4 (n=72)	4 (n=72)
<i>lin-35; spr-1; lin-12</i> (RNAi)	24 (n=45)	62 (n=45)

All RNAi experiments were carried out using injection methods. The *fld6* allele of *spr-1* was used in all experiments.

<sup>a</sup> Phenotypes were scored per gonad arm.

<sup>b</sup> *spr-1(fld6)* was linked to *unc-76(e911)*.

<sup>c</sup> *sel-12(ar171)* was linked to *unc-1(e538)*.

<sup>d</sup> Actual strain was of genotype *lin-35; spr-1; lin-12*(RNAi); *kuEx119*, which is rescued for the *lin-35* mutant defect.

showed little or no expression of the Pro phenotype (Table 4). In addition, adult triple mutants often harbored residual bodies (from spermatocytes) in the proximal gonad region (Fig. 6F; Table 4). Residual bodies are a relatively short-lived bi-product of spermatogenesis and are typically absent in adults. Residual bodies were not observed in wild-type adults, although they were observed at somewhat elevated frequencies in most double-mutant combinations (Table 4).

The Pro phenotype is defined by abnormal cell divisions in the proximal region of the adult germline and is discernible as a mass of densely packed mitotic nuclei (Seydoux et al., 1990). This phenotype has been reported to arise by several distinct mechanisms including the dedifferentiation of developing (meiotic) spermatocytes into mitotically dividing cells (Subramaniam and Seydoux, 2003). In addition, careful analysis has shown the Pro phenotype to result indirectly from delays in the initial entry of proximal germ cells into meiosis (Pepper et al., 2003a,b; Killian and Hubbard, 2004, 2005). This delay can occur when the germline fails to proliferate sufficiently during larval development, such that the proximal germ cells remain under the mitosis-promoting influence of the distal tip cell (via LAG-2/Delta and GLP-1/Notch signaling). This failure of the proximal germ cells to enter meiosis in a timely manner renders them susceptible to the mitosis-promoting influence of the proximal sheath cells (Sh2–5) that come into contact with the proximal germ cells during the mid-L4 stage (Killian and Hubbard, 2005). Therefore, it is critical that germ cells enter meiosis prior to the birth of Sh2–5, as subtle delays can lead to maintenance of a mitotic state and the generation of proximal tumors.

Several features of the meiotic entry delay mechanism were consistent with our observations of the triple mutants including a highly penetrant reduction in the proliferation capacity of the triple-mutant germline. In addition, it has been shown that *lin-12* LOF results in delays in the timing of initial meiosis (Killian and Hubbard, 2005; Killian and Hubbard, 2004) and that *lin-12* null mutants form proximal tumors and contain adult-stage spermatocytes (Seydoux et al., 1990). In contrast, *puf-8(RNAi)*, which leads to highly penetrant proximal tumors via the spermatocyte dedifferentiation pathway, does not typically affect germline proliferation (Subramaniam and Seydoux, 2003). Furthermore, other phenotypes associated with *puf-8* LOF that occur as a consequence of meiotic defects were not observed in the double or triple mutants examined (data not shown; Subramaniam and Seydoux, 2003). Finally, the presence of residual bodies in triple mutant adults is consistent with a delay in the initiation of meiosis and in the subsequent induction of spermatogenesis.

To test for delays in the timing of initial meiosis in *lin-35; spr-1; hop-1(RNAi)* and *lin-35; spr-1; lin-12(RNAi)* triple-mutant animals, we examined gonads by DAPI staining at the mid-L4 stage, at which time a substantial proportion of wild-type germ cells have normally entered meiosis (Hubbard and Greenstein, 2005). We found that in contrast to wild type as well as all possible double-mutant combinations, triple mutants were specifically defective in meiotic entry (Table 5; Figs. 6I, J). These results correlate precisely with the expression of the Pro

Table 5

Germline meiotic progression at the mid-L4 stage

Genotype	Mitotic	Transition	Pachytene	<i>n</i>
N2	148±24	19±4	56±24	8
<i>lin-35; hop-1(RNAi)</i>	95±13	12±5	38±5	9
<i>lin-35; lin-12(RNAi)</i>	85±15	10±2	46±7	8
<i>spr-1; hop-1(RNAi)<sup>a</sup></i>	93±11	25±5	38±6	10
<i>spr-1; lin-12(RNAi)<sup>a</sup></i>	85±16	20±6	29±5	10
<i>lin-35; spr-1</i>	37±6	8±2	31±9	7
<i>lin-35; spr-1; hop-1(RNAi)</i>	48±11	5±3 <sup>b</sup>	11±10 <sup>c</sup>	8
<i>lin-35; spr-1; lin-12(RNAi)</i>	47±14	5±3 <sup>d</sup>	16±13 <sup>e</sup>	17

All RNAi experiments were carried out using injection methods. The *fd6* allele of *spr-1* was used in all experiments. *n* indicates the number of gonad arms scored.

<sup>a</sup> Scored animals contained the *lin-35(n745)* mutation together with the *lin-35* rescuing array *kuEx119*.

<sup>b</sup> 3/8 gonad arms contained no transition-stage nuclei. *p*-value based on *t* test (relative to *lin-35; spr-1*) was <0.01.

<sup>c</sup> 2/8 gonad arms contained no pachytene-stage nuclei. *p*-value based on *t* test (relative to *lin-35; spr-1*) was <<0.01.

<sup>d</sup> 8/17 gonad arms contained no transition-stage nuclei. *p*-value based on *t* test (relative to *lin-35; spr-1*) was <<0.001.

<sup>e</sup> 8/17 gonad arms contained no pachytene-stage nuclei. *p*-value based on *t* test (relative to *lin-35; spr-1*) was <<0.001.

phenotype in the triple-mutant, but not the double-mutant, combinations (Table 4). Furthermore, these findings are highly consistent with previous studies linking delays in the timing of initial meiosis to the Pro phenotype (Pepper et al., 2003a,b; Killian and Hubbard, 2004, 2005). In particular, we note that *lin-35; lin-12(RNAi)* animals showed neither a pronounced meiotic entry delay nor a Pro phenotype, indicating that our level of *lin-12* inactivation was not sufficient on its own to induce obvious germline defects (Fig. 6I; Table 4); *lin-35; lin-12(RNAi)* animals did display the Egl phenotype, and 2/15 animals assayed contained two anchor cells (data not shown), consistent with a partial loss of *lin-12* function. Thus, *lin-35; spr-1* mutants are highly sensitized to the effects of *lin-12* LOF on germline development. This result is reminiscent of previous findings showing that ablation of sheath cell pair 1 (Sh1), which leads to both a meiotic entry delay and germline underproliferation, sensitizes the animals to slight increases in GLP-1/Notch activity, effectively resulting in a synthetic Pro phenotype.

## Discussion

### *lin-35/Rb* and *spr-1/CoREST* function redundantly during *C. elegans* development

We found that *lin-35* and *spr-1* redundantly control several aspects of somatic gonad and germline development. With respect to development of the vulva, our results demonstrate that *lin-35* and *spr-1* coordinately promote the normal ingress of vulval cells during the late L3 and L4 stages of development (Table 1; Figs. 2, 3). This phenotype is superficially similar to that of the *sqv* mutants, which act in a common pathway to promote chondroitin biosynthesis (reviewed by Bulik and Robbins, 2002). Although our findings

do not support a model whereby chondroitin biosynthesis or localization is grossly altered in the double mutants (as is the case for the *sqv* mutants; Fig. 5), we cannot rule out the possibility that very subtle differences in chondroitin levels, processing, or conjugation to specific proteoglycan core components may play a role in the observed phenotype. Nevertheless, clear qualitative differences in the vulval morphologies of *lin-35*; *spr-1* and the *sqv* mutants, along with the normal localization pattern of chondroitin observed in *lin-35*; *spr-1* vulvae, argue against chondroitin-related defects as being causative to the *lin-35*; *spr-1* vulval phenotype.

We have also shown a role for *lin-35* and *spr-1* in germline proliferation and in the prevention of proximal germline tumors when LIN-12/Notch signaling is compromised (Figs. 4, 6; Tables 4, 5). Based on previous published studies (Killian and Hubbard, 2004, 2005), we hypothesize that *lin-35* and *spr-1* contribute to the Pro phenotype through their roles in redundantly promoting germline proliferation (also see results). At present, our data do not indicate whether *lin-35* and *spr-1* promote germline proliferation autonomously or via the soma. Nevertheless, our studies strongly imply that the Pro phenotype of *lin-35*; *spr-1*; *lin-12(RNAi)* and *lin-35*; *spr-1*; *hop-1(RNAi)* triple mutants results from a delay in the timing of initial meiosis, consistent with previous studies (Pepper et al., 2003a,b; Killian and Hubbard, 2004, 2005). Curiously, loss of *lin-35* can also suppress the Pro phenotype of *pro-1* mutants by partially alleviating defects due to rRNA processing deficiencies (Voutev et al., 2006). Thus, depending on developmental context and strain background, *lin-35* can act as either a suppressor or enhancer of proximal germline proliferation.

#### Redundancy among transcriptional regulators

Genetic redundancy, which implies an overlap in the functions of the encoded protein products, can occur through a myriad of mechanisms. For example, the synthetic hyperproliferative phenotype of *lin-35*; *fzr-1* mutants results from a failure to repress the expression of G1 cyclins adequately (Fay et al., 2002). In this case, LIN-35, acting as a transcriptional repressor, and FZR-1, functioning as a component of the APC ubiquitin ligase complex, act at distinct points (transcriptional versus post-translational) to control the protein levels of a mutual target. In contrast, as described in the Introduction, LIN-35 acting together with other SynMuv genes specifically represses *lin-3* at the level of transcription (Cui et al., 2006). Although the precise molecular functions of the Class A SynMuv genes are not known, these proteins localize to the nucleus and are likely to function as transcriptional regulators (Clark et al., 1994; Huang et al., 1994; Davison et al., 2005).

It is of interest to note that of the seven genes identified through our *lin-35* synthetic screen, four function as regulators of transcription (*spr-1*; Bender et al., 2004; Cui et al., 2004; D.S.F. and J.D. McEnerney, unpublished data). Furthermore, mutations in *gon-14* are also synthetic with *lin-35*, and GON-14 contains a putative THAP DNA-binding domain and

localizes to the nucleus (Chesney et al., 2006). Thus, although transcriptional regulators account for less than 8% of encoded genes in *C. elegans*, they are strongly over-represented among the group of known *lin-35* synthetic interactors. This observation is consistent with findings from a large-scale synthetic screen in *S. cerevisiae* showing that genes encoding proteins with similar molecular functions (based on gene ontologies) are more likely to display genetic redundancy than are genes with dissimilar functions (Tong et al., 2004). Thus, a useful (though imperfect) predictor for functional redundancy in metazoa may be based on proteins that have similar molecular functions.

#### The role of pocket proteins in tumor suppression

In this study, we have identified an additional role for *lin-35* in epithelial cell movement and ingression. Although we have yet to identify the underlying basis for this phenotype, straightforward possibilities include reduced or altered adhesion properties of the migrating vulval cells or defects in cell polarity that may lead to a diminution of cell movements. Together with our previous observations demonstrating a role for *lin-35* in controlling cell orientation and polarity during pharyngeal morphogenesis (Fay et al., 2003, 2004), these results suggest that *lin-35* controls several properties of cells that are known to be specifically derailed in mammalian metastatic cancers (reviewed by Christofori, 2006).

It is possible that similar functions for Rb family members also exist in mammals but have not been observed to date because of functional overlap between the Rb family members, or as is the case in *C. elegans*, because of genetic redundancy with independent pathways. Additional tumor-suppressive functions may further explain why the Rb pathway is functionally inactivated in most or all human cancers (Sherr, 1996, 2004; Sherr and McCormick, 2002). Furthermore, a role for Rb in tumor suppression beyond cell cycle control is supported by the finding that loss of cell cycle control alone is not sufficient to predispose cells of the retina to form Retinoblastomas (Nakayama et al., 1996; Levine et al., 2000; Dyer and Cepko, 2001; Cunningham et al., 2002; reviewed by Bremner et al., 2004). We speculate that genes identified as showing synthetic interactions with *lin-35* may function in certain contexts as tumor suppressors in mammals. Our identification of *spr-1/CoREST*, which functions in mammals as the co-partner of the REST tumor suppressor protein, lends credence to this possibility. Another gene identified by our screen, *fzr-1/Cdh1*, is strongly downregulated in murine lymphoma cells, and transgenic expression of murine *fzr-1* in these cells reverts their tumorous growth properties (Wang et al., 2000). Finally, the recent finding that LIN-35 redundantly represses expression of the EGF family member LIN-3 suggests that suppression of paracrine growth factor signaling may be another mechanism by which Rb family members inhibit cell growth and thereby function to prevent tumorigenesis (Cui et al., 2006). Thus, the analysis of *lin-35* functions during development may provide valuable insights into novel mechanisms of tumor suppression by the Rb family.

## Acknowledgments

We are especially indebted to Jane Hubbard for helpful suggestions and comments and to Amy Fluet for input on the manuscript. We thank Michael Stern, Jeff Hardin, Bill Mohler, Wendy Hanna-Rose, and David Greenstein for reagents. This work was supported by a Research Scholar Grant from the American Cancer Society (RSG-03-035-01-DDC) and GM066868 (to D.S.F) and G33063 (to J.D.E) from the National Institutes of Health.

## References

- Ahringer, J., 2005. Reverse Genetics, WormBook (The. *C. elegans*. Research Community, Ed.). <http://www.wormbook.org/>.
- Andres, M.E., Burger, C., Peral-Rubio, M.J., Battaglioli, E., Anderson, M.E., Grimes, J., Dallman, J., Ballas, N., Mandel, G., 1999. CoREST: a functional corepressor required for regulation of neural-specific gene expression. *Proc. Natl. Acad. Sci. U. S. A.* 96, 9873–9878.
- Balciunaitė, E., Spektor, A., Lents, N.H., Cam, H., Te Riele, H., Scime, A., Rudnicki, M.A., Young, R., Dynlacht, B.D., 2005. Pocket protein complexes are recruited to distinct targets in quiescent and proliferating cells. *Mol. Cell. Biol.* 25, 8166–8178.
- Bender, A.M., Wells, O., Fay, D.S., 2004. lin-35/Rb and xnp-1/ATR-X function redundantly to control somatic gonad development in *C. elegans*. *Dev. Biol.* 273, 335–349.
- Black, E.P., Huang, E., Dressman, H., Rempel, R., Laakso, N., Asa, S.L., Ishida, S., West, M., Nevins, J.R., 2003. Distinct gene expression phenotypes of cells lacking Rb and Rb family members. *Cancer Res.* 63, 3716–3723.
- Boxem, M., van den Heuvel, S., 2001. lin-35 Rb and cki-1 Cip/Kip cooperate in developmental regulation of G1 progression in *C. elegans*. *Development* 128, 4349–4359.
- Boyer, L.A., Langer, M.R., Crowley, K.A., Tan, S., Denu, J.M., Peterson, C.L., 2002. Essential role for the SANT domain in the functioning of multiple chromatin remodeling enzymes. *Mol. Cell* 10, 935–942.
- Bremner, R., Chen, D., Pacal, M., Livne-Bar, I., Agochiya, M., 2004. The RB protein family in retinal development and retinoblastoma: new insights from new mouse models. *Dev. Neurosci.* 26, 417–434.
- Bulik, D.A., Robbins, P.W., 2002. The *Caenorhabditis elegans* sqv genes and functions of proteoglycans in development. *Biochim. Biophys. Acta* 1573, 247–257.
- Bulik, D.A., Wei, G., Toyoda, H., Kinoshita-Toyoda, A., Waldrip, W.R., Esko, J.D., Robbins, P.W., Selleck, S.B., 2000. sqv-3,-7, and-8, a set of genes affecting morphogenesis in *Caenorhabditis elegans*, encode enzymes required for glycosaminoglycan biosynthesis. *Proc. Natl. Acad. Sci. U. S. A.* 97, 10838–10843.
- Burdine, R.D., Branda, C.S., Stern, M.J., 1998. EGL-17(FGF) expression coordinates the attraction of the migrating sex myoblasts with vulval induction in *C. elegans*. *Development* 125, 1083–1093.
- Cardoso, C., Couillault, C., Mignon-Ravix, C., Millet, A., Ewbank, J.J., Fontes, M., Pujol, N., 2005. XNP-1/ATR-X acts with RB, HP1 and the NuRD complex during larval development in *C. elegans*. *Dev. Biol.* 278, 49–59.
- Ceol, C.J., Horvitz, H.R., 2001. dpl-1 DP and efl-1 E2F act with lin-35 Rb to antagonize Ras signaling in *C. elegans* vulval development. *Mol. Cell* 7, 461–473.
- Ceol, C.J., Horvitz, H.R., 2004. A new class of *C. elegans* synMuv genes implicates a Tip60/NuA4-like HAT complex as a negative regulator of Ras signaling. *Dev. Cell* 6, 563–576.
- Chesney, M.A., Kidd III, A.R., Kimble, J., 2006. gon-14 functions with class B and class C synthetic multivulva genes to control larval growth in *Caenorhabditis elegans*. *Genetics* 172, 915–928.
- Christofori, G., 2006. New signals from the invasive front. *Nature* 441, 444–450.
- Clark, S.G., Lu, X., Horvitz, H.R., 1994. The *Caenorhabditis elegans* locus lin-15, a negative regulator of a tyrosine kinase signaling pathway, encodes two different proteins. *Genetics* 137, 987–997.
- Classon, M., Dyson, N., 2001. p107 and p130: versatile proteins with interesting pockets. *Exp. Cell Res.* 264, 135–147.
- Cui, M., Fay, D.S., Han, M., 2004. lin-35/Rb cooperates with the SWI/SNF complex to control *Caenorhabditis elegans* larval development. *Genetics* 167, 1177–1185.
- Cui, M., Chen, J., Myers, T.R., Hwang, B.J., Sternberg, P.W., Greenwald, I., Han, M., 2006. SynMuv genes redundantly inhibit lin-3/EGF expression to prevent inappropriate vulval induction in *C. elegans*. *Dev. Cell* 10, 667–672.
- Cunningham, J.J., Levine, E.M., Zindy, F., Goloubeva, O., Roussel, M.F., Smeyne, R.J., 2002. The cyclin-dependent kinase inhibitors p19(Ink4d) and p27(Kip1) are coexpressed in select retinal cells and act cooperatively to control cell cycle exit. *Mol. Cell Neurosci.* 19, 359–374.
- Davison, E.M., Harrison, M.M., Walhout, A.J., Vidal, M., Horvitz, H.R., 2005. lin-8, which antagonizes *Caenorhabditis elegans* Ras-mediated vulval induction, encodes a novel nuclear protein that interacts with the LIN-35 Rb protein. *Genetics* 171, 1017–1031.
- de Bruin, A., Wu, L., Saavedra, H.I., Wilson, P., Yang, Y., Rosol, T.J., Weinstein, M., Robinson, M.L., Leone, G., 2003. Rb function in extraembryonic lineages suppresses apoptosis in the CNS of Rb-deficient mice. *Proc. Natl. Acad. Sci. U. S. A.* 100, 6546–6551.
- Dimova, D.K., Stevaux, O., Frolov, M.V., Dyson, N.J., 2003. Cell cycle-dependent and cell cycle-independent control of transcription by the *Drosophila* E2F/RB pathway. *Genes Dev.* 17, 2308–2320.
- Duerr, J.S., 2005. Immunohistochemistry, WormBook (The. *C. elegans*. Research Community, Ed.). <http://www.wormbook.org/>.
- Dyer, M.A., Cepko, C.L., 2001. The p57Kip2 cyclin kinase inhibitor is expressed by a restricted set of amacrine cells in the rodent retina. *J. Comp. Neurol.* 429, 601–614.
- Eimer, S., Lakowski, B., Donhauser, R., Baumeister, R., 2002. Loss of spr-5 bypasses the requirement for the *C. elegans* presenilin sel-12 by derepressing hop-1. *Embo J.* 21, 5787–5796.
- Evans, T.C., 2005. Transformation and Microinjection, WormBook (The. *C. elegans*. Research Community, Ed.). <http://www.wormbook.org/>.
- Fay, D.S., 2005. The cell cycle and development: lessons from *C. elegans*. *Semin. Cell Dev. Biol.* 16, 397–406.
- Fay, D.S., 2006. Genetic Mapping and Manipulation, WormBook (The. *C. elegans*. Research Community, Ed.). <http://www.wormbook.org/>.
- Fay, D.S., Han, M., 2000. The synthetic multivulval genes of *C. elegans*: functional redundancy, Ras-antagonism, and cell fate determination. *Genesis* 26, 279–284.
- Fay, D.S., Keenan, S., Han, M., 2002. fzf-1 and lin-35/Rb function redundantly to control cell proliferation in *C. elegans* as revealed by a nonbiased synthetic screen. *Genes Dev.* 16, 503–517.
- Fay, D.S., Large, E., Han, M., Darland, M., 2003. lin-35/Rb and ubc-18, an E2 ubiquitin-conjugating enzyme, function redundantly to control pharyngeal morphogenesis in *C. elegans*. *Development* 130, 3319–3330.
- Fay, D.S., Qiu, X., Large, E., Smith, C.P., Mango, S., Johanson, B.L., 2004. The coordinate regulation of pharyngeal development in *C. elegans* by lin-35/Rb, pha-1, and ubc-18. *Dev. Biol.* 271, 11–25.
- Ferguson, E.L., Horvitz, H.R., 1989. The multivulva phenotype of certain *Caenorhabditis elegans* mutants results from defects in two functionally redundant pathways. *Genetics* 123, 109–121.
- Greenwald, I., 2005. LIN-12/Notch signaling in *C. elegans*, WormBook (The. *C. elegans*. Research Community, Ed.). <http://www.wormbook.org/>.
- Hall, D.H., Winfrey, V.P., Blaeuer, G., Hoffman, L.H., Furuta, T., Rose, K.L., Hobert, O., Greenstein, D., 1999. Ultrastructural features of the adult hermaphrodite gonad of *Caenorhabditis elegans*: relations between the germ line and soma. *Dev. Biol.* 212, 101–123.
- Hanna-Rose, W., Han, M., 1999. COG-2, a sox domain protein necessary for establishing a functional vulval-uterine connection in *Caenorhabditis elegans*. *Development* 126, 169–179.
- Harbour, J.W., Dean, D.C., 2000a. Rb function in cell-cycle regulation and apoptosis. *Nat. Cell Biol.* 2, E65–E67.
- Harbour, J.W., Dean, D.C., 2000b. The Rb/E2F pathway: expanding roles and emerging paradigms. *Genes Dev.* 14, 2393–2409.
- Herman, T., Horvitz, H.R., 1999. Three proteins involved in *Caenorhabditis*

- elegans* vulval invagination are similar to components of a glycosylation pathway. *Proc. Natl. Acad. Sci. U. S. A.* 96, 974–979.
- Herman, T., Hartwig, E., Horvitz, H.R., 1999. sqv mutants of *Caenorhabditis elegans* are defective in vulval epithelial invagination. *Proc. Natl. Acad. Sci. U. S. A.* 96, 968–973.
- Hsieh, J., Liu, J., Kostas, S.A., Chang, C., Sternberg, P.W., Fire, A., 1999. The RING finger/B-box factor TAM-1 and a retinoblastoma-like protein LIN-35 modulate context-dependent gene silencing in *Caenorhabditis elegans*. *Genes Dev.* 13, 2958–2970.
- Huang, L.S., Tzou, P., Sternberg, P.W., 1994. The lin-15 locus encodes two negative regulators of *Caenorhabditis elegans* vulval development. *Mol. Biol. Cell* 5, 395–411.
- Hubbard, E.J., Greenstein, D., 2005. Introduction to the Germline, WormBook. (The *C. elegans* Research Community, Ed.). <http://www.wormbook.org/>.
- Humphrey, G.W., Wang, Y., Russanova, V.R., Hirai, T., Qin, J., Nakatani, Y., Howard, B.H., 2001. Stable histone deacetylase complexes distinguished by the presence of SANT domain proteins CoREST/kiaa0071 and Mta-L1. *J. Biol. Chem.* 276, 6817–6824.
- Hwang, H.Y., Horvitz, H.R., 2002a. The *Caenorhabditis elegans* vulval morphogenesis gene sqv-4 encodes a UDP-glucose dehydrogenase that is temporally and spatially regulated. *Proc. Natl. Acad. Sci. U. S. A.* 99, 14224–14229.
- Hwang, H.Y., Horvitz, H.R., 2002b. The SQV-1 UDP-glucuronic acid decarboxylase and the SQV-7 nucleotide-sugar transporter may act in the Golgi apparatus to affect *Caenorhabditis elegans* vulval morphogenesis and embryonic development. *Proc. Natl. Acad. Sci. U. S. A.* 99, 14218–14223.
- Hwang, H.Y., Olson, S.K., Brown, J.R., Esko, J.D., Horvitz, H.R., 2003a. The *Caenorhabditis elegans* genes sqv-2 and sqv-6, which are required for vulval morphogenesis, encode glycosaminoglycan galactosyltransferase II and xylosyltransferase. *J. Biol. Chem.* 278, 11735–11738.
- Hwang, H.Y., Olson, S.K., Esko, J.D., Horvitz, H.R., 2003b. *Caenorhabditis elegans* early embryogenesis and vulval morphogenesis require chondroitin biosynthesis. *Nature* 423, 439–443.
- Iwamoto, R., Mekada, E., 2006. ErbB and HB-EGF signaling in heart development and function. *Cell Struct. Funct.* 31, 1–14.
- Jarriault, S., Greenwald, I., 2002. Suppressors of the egg-laying defective phenotype of sel-12 presenilin mutants implicate the CoREST corepressor complex in LIN-12/Notch signaling in *C. elegans*. *Genes Dev.* 16, 2713–2728.
- Kaelin Jr., W.G., 1999. Functions of the retinoblastoma protein. *BioEssays* 21, 950–958.
- Killian, D.J., Hubbard, E.J., 2004. *C. elegans* pro-1 activity is required for soma/germline interactions that influence proliferation and differentiation in the germ line. *Development* 131, 1267–1278.
- Killian, D.J., Hubbard, E.J., 2005. *Caenorhabditis elegans* germline patterning requires coordinated development of the somatic gonadal sheath and the germ line. *Dev. Biol.* 279, 322–335.
- Kitagawa, H., Egusa, N., Tamura, J.I., Kusche-Gullberg, M., Lindahl, U., Sugahara, K., 2001. rib-2, a *Caenorhabditis elegans* homolog of the human tumor suppressor EXT genes encodes a novel alpha1,4-N-acetylglucosaminyltransferase involved in the biosynthetic initiation and elongation of heparan sulfate. *J. Biol. Chem.* 276, 4834–4838.
- Krutzfeldt, M., Ellis, M., Weekes, D.B., Bull, J.J., Eilers, M., Vivanco, M.D., Sellers, W.R., Mittnacht, S., 2005. Selective ablation of retinoblastoma protein function by the RET finger protein. *Mol. Cell* 18, 213–224.
- Lakowski, B., Eimer, S., Gobel, C., Bottcher, A., Wagler, B., Baumeister, R., 2003. Two suppressors of sel-12 encode C2H2 zinc-finger proteins that regulate presenilin transcription in *Caenorhabditis elegans*. *Development* 130, 2117–2128.
- Lee, M.G., Wynder, C., Cooch, N., Shiekhhattar, R., 2005. An essential role for CoREST in nucleosomal histone 3 lysine 4 demethylation. *Nature* 437, 432–435.
- Levine, E.M., Close, J., Fero, M., Ostrovsky, A., Reh, T.A., 2000. p27(Kip1) regulates cell cycle withdrawal of late multipotent progenitor cells in the mammalian retina. *Dev. Biol.* 219, 299–314.
- Levitan, D., Greenwald, I., 1995. Facilitation of lin-12-mediated signalling by sel-12, a *Caenorhabditis elegans* S182 Alzheimer's disease gene. *Nature* 377, 351–354.
- Li, X., Greenwald, I., 1997. HOP-1, a *Caenorhabditis elegans* presenilin, appears to be functionally redundant with SEL-12 presenilin and to facilitate LIN-12 and GLP-1 signaling. *Proc. Natl. Acad. Sci. U. S. A.* 94, 12204–12209.
- Lu, X., Horvitz, H.R., 1998. lin-35 and lin-53, two genes that antagonize a *C. elegans* Ras pathway, encode proteins similar to Rb and its binding protein RbAp48. *Cell* 95, 981–991.
- MacPherson, D., Sage, J., Crowley, D., Trumpp, A., Bronson, R.T., Jacks, T., 2003. Conditional mutation of Rb causes cell cycle defects without apoptosis in the central nervous system. *Mol. Cell. Biol.* 23, 1044–1053.
- Markey, M.P., Angus, S.P., Strobeck, M.W., Williams, S.L., Gunawardena, R.W., Aronow, B.J., Knudsen, E.S., 2002. Unbiased analysis of RB-mediated transcriptional repression identifies novel targets and distinctions from E2F action. *Cancer Res.* 62, 6587–6597.
- McCarter, J., Bartlett, B., Dang, T., Schedl, T., 1997. Soma-germ cell interactions in *Caenorhabditis elegans*: multiple events of hermaphrodite germline development require the somatic sheath and spermathecal lineages. *Dev. Biol.* 181, 121–143.
- Mizuguchi, S., Uyama, T., Kitagawa, H., Nomura, K.H., Dejima, K., Gengyo-Ando, K., Mitani, S., Sugahara, K., Nomura, K., 2003. Chondroitin proteoglycans are involved in cell division of *Caenorhabditis elegans*. *Nature* 423, 443–448.
- Mohler, W.A., Simske, J.S., Williams-Masson, E.M., Hardin, J.D., White, J.G., 1998. Dynamics and ultrastructure of developmental cell fusions in the *Caenorhabditis elegans* hypodermis. *Curr. Biol.* 8, 1087–1090.
- Morio, H., Honda, Y., Toyoda, H., Nakajima, M., Kurosawa, H., Shirasawa, T., 2003. EXT gene family member rib-2 is essential for embryonic development and heparan sulfate biosynthesis in *Caenorhabditis elegans*. *Biochem. Biophys. Res. Commun.* 301, 317–323.
- Morris, E.J., Dyson, N.J., 2001. Retinoblastoma protein partners. *Adv. Cancer Res.* 82, 1–54.
- Muller, H., Bracken, A.P., Vernell, R., Moroni, M.C., Christians, F., Grassilli, E., Prosperini, E., Vigo, E., Oliner, J.D., Helin, K., 2001. E2Fs regulate the expression of genes involved in differentiation, development, proliferation, and apoptosis. *Genes Dev.* 15, 267–285.
- Myster, D.L., Bonnette, P.C., Duronio, R.J., 2000. A role for the DP subunit of the E2F transcription factor in axis determination during *Drosophila* oogenesis. *Development* 127, 3249–3261.
- Nakayama, K., Ishida, N., Shirane, M., Inomata, A., Inoue, T., Shishido, N., Horii, I., Loh, D.Y., Nakayama, K., 1996. Mice lacking p27(Kip1) display increased body size, multiple organ hyperplasia, retinal dysplasia, and pituitary tumors. *Cell* 85, 707–720.
- Olson, S.K., Bishop, J.R., Yates, J.R., Oegema, K., Esko, J.D., 2006. Identification of novel chondroitin proteoglycans in *Caenorhabditis elegans*: embryonic cell division depends on CPG-1 and CPG-2. *J. Cell Biol.* 173, 985–994.
- Page, B.D., Guedes, S., Waring, D., Priess, J.R., 2001. The *C. elegans* E2F- and DP-related proteins are required for embryonic asymmetry and negatively regulate Ras/MAPK signaling. *Mol. Cell* 7, 451–460.
- Pepper, A.S., Lo, T.W., Killian, D.J., Hall, D.H., Hubbard, E.J., 2003a. The establishment of *Caenorhabditis elegans* germline pattern is controlled by overlapping proximal and distal somatic gonad signals. *Dev. Biol.* 259, 336–350.
- Pepper, A.S., Killian, D.J., Hubbard, E.J., 2003b. Genetic analysis of *Caenorhabditis elegans* glp-1 mutants suggests receptor interaction or competition. *Genetics* 163, 115–132.
- Polager, S., Kalma, Y., Berkovich, E., Ginsberg, D., 2002. E2Fs up-regulate expression of genes involved in DNA replication, DNA repair and mitosis. *Oncogene* 21, 437–446.
- Powell, A.K., Yates, E.A., Fernig, D.G., Turnbull, J.E., 2004. Interactions of heparin/heparan sulfate with proteins: appraisal of structural factors and experimental approaches. *Glycobiology* 14, 17R–30R.
- Ruiz, S., Segrelles, C., Bravo, A., Santos, M., Perez, P., Leis, H., Jorcano, J.L., Paramio, J.M., 2003. Abnormal epidermal differentiation and impaired epithelial-mesenchymal tissue interactions in mice lacking the retinoblastoma relatives p107 and p130. *Development* 130, 2341–2353.
- Sage, C., Huang, M., Karimi, K., Gutierrez, G., Vollrath, M.A., Zhang, D.S.,

- Garcia-Anoveros, J., Hinds, P.W., Corwin, J.T., Corey, D.P., Chen, Z.Y., 2005. Proliferation of functional hair cells in vivo in the absence of the retinoblastoma protein. *Science* 307, 1114–1118.
- Seydoux, G., Schedl, T., Greenwald, I., 1990. Cell–cell interactions prevent a potential inductive interaction between soma and germline in *C. elegans*. *Cell* 61, 939–951.
- Sherr, C.J., 1996. Cancer cell cycles. *Science* 274, 1672–1677.
- Sherr, C.J., 2004. Principles of tumor suppression. *Cell* 116, 235–246.
- Sherr, C.J., McCormick, F., 2002. The RB and p53 pathways in cancer. *Cancer Cell* 2, 103–112.
- Sternberg, P.W., 2005. Vulval Development, WormBook (The *C. elegans* Research Community, Ed.). <http://www.wormbook.org/>.
- Stiernagle, T., 2005. Maintenance of *C. elegans*, WormBook (The *C. elegans* Research Community, Ed.). <http://www.wormbook.org/>.
- Subramaniam, K., Seydoux, G., 2003. Dedifferentiation of primary spermatocytes into germ cell tumors in *C. elegans* lacking the pumilio-like protein PUF-8. *Curr. Biol.* 13, 134–139.
- Sundaram, M., Greenwald, I., 1993. Genetic and phenotypic studies of hypomorphic *lin-12* mutants in *Caenorhabditis elegans*. *Genetics* 135, 755–763.
- Suzuki, A., Hemmati-Brivanlou, A., 2000. *Xenopus* embryonic E2F is required for the formation of ventral and posterior cell fates during early embryogenesis. *Mol. Cell* 5, 217–229.
- Takahashi, C., Contreras, B., Bronson, R.T., Loda, M., Ewen, M.E., 2004. Genetic interaction between Rb and K-ras in the control of differentiation and tumor suppression. *Mol. Cell Biol.* 24, 10406–10415.
- Tong, A.H., Lesage, G., Bader, G.D., Ding, H., Xu, H., Xin, X., Young, J., Berri, G.F., Brost, R.L., Chang, M., Chen, Y., Cheng, X., Chua, G., Friesen, H., Goldberg, D.S., Haynes, J., Humphries, C., He, G., Hussein, S., Ke, L., Krogan, N., Li, Z., Levinson, J.N., Lu, H., Menard, P., Munyana, C., Parsons, A.B., Ryan, O., Tonikian, R., Roberts, T., Sdicu, A.M., Shapiro, J., Sheikh, B., Suter, B., Wong, S.L., Zhang, L.V., Zhu, H., Burd, C.G., Munro, S., Sander, C., Rine, J., Greenblatt, J., Peter, M., Bretscher, A., Bell, G., Roth, F.P., Brown, G.W., Andrews, B., Bussey, H., Boone, C., 2004. Global mapping of the yeast genetic interaction network. *Science* 303, 808–813.
- Voutev, C., Killian, D.J., Ahn, J.H., Hubbard, E.J., Braun, J., 2006. Alterations in ribosome biogenesis cause specific defects in *C. elegans* hermaphrodite gonadogenesis. *Dev. Biol.* 298, 45–58.
- Wang, C.X., Fisk, B.C., Wadehra, M., Su, H., Braun, J., 2000. Overexpression of murine fizzy-related (*fzr*) increases natural killer cell-mediated cell death and suppresses tumor growth. *Blood* 96, 259–263.
- Wang, D., Kennedy, S., Conte Jr., D., Kim, J.K., Gabel, H.W., Kamath, R.S., Mello, C.C., Ruvkun, G., 2005. Somatic misexpression of germline P granules and enhanced RNA interference in retinoblastoma pathway mutants. *Nature* 436, 593–597.
- Westbrook, T.F., Martin, E.S., Schlabach, M.R., Leng, Y., Liang, A.C., Feng, B., Zhao, J.J., Roberts, T.M., Mandel, G., Hannon, G.J., Depinho, R.A., Chin, L., Elledge, S.J., 2005. A genetic screen for candidate tumor suppressors identifies REST. *Cell* 121, 837–848.
- Westlund, B., Parry, D., Clover, R., Basson, M., Johnson, C.D., 1999. Reverse genetic analysis of *Caenorhabditis elegans* presenilins reveals redundant but unequal roles for *sel-12* and *hop-1* in Notch-pathway signaling. *Proc. Natl. Acad. Sci. U. S. A.* 96, 2497–2502.
- Wikenheiser-Brokamp, K.A., 2004. Rb family proteins differentially regulate distinct cell lineages during epithelial development. *Development* 131, 4299–4310.
- Wikenheiser-Brokamp, K.A., 2006. Retinoblastoma family proteins: insights gained through genetic manipulation of mice. *Cell Mol. Life Sci.* 63, 767–780.
- Wu, L., de Bruin, A., Saavedra, H.I., Starovic, M., Trimboli, A., Yang, Y., Opavska, J., Wilson, P., Thompson, J.C., Ostrowski, M.C., Rosol, T.J., Woollett, L.A., Weinstein, M., Cross, J.C., Robinson, M.L., Leone, G., 2003. Extra-embryonic function of Rb is essential for embryonic development and viability. *Nature* 421, 942–947.
- You, A., Tong, J.K., Grozinger, C.M., Schreiber, S.L., 2001. CoREST is an integral component of the CoREST-human histone deacetylase complex. *Proc. Natl. Acad. Sci. U. S. A.* 98, 1454–1458.